Applied Energy xxx (2016) xxx–xxx

Contents lists available at ScienceDirect

Applied Energy

journal homepage: www.elsevier.com/locate/apenergy

Working fluid selection and electrical performance optimisation of a domestic solar-ORC combined heat and power system for year-round operation in the UK

James Freeman, Klaus Hellgardt, Christos N. Markides *

Clean Energy Processes (CEP) Laboratory, Department of Chemical Engineering, Imperial College London, South Kensington Campus, London SW7 2AZ, UK

HIGHLIGHTS

- A domestic solar combined heat & power (S-CHP) system is optimised for maximum electrical output in the UK.
- The S-CHP system comprises a solar collector array, an ORC engine and a working fluid buffer vessel.
- A working fluid and evaporation temperature optimisation are performed for an annual operation period.
- A single-stage and a two-stage collector array configuration are compared.
- An optimum annual-average electrical power of 122 W for the two-stage configuration is reported.

ARTICLE INFO

Article history:
Received 18 October 2015
Received in revised form 30 March 2016
Accepted 10 April 2016
Available online xxxx

Keywords:
Renewable technologies
Solar power
Solar thermal
Domestic
Combined heat and power
Organic Rankine cycle

ABSTRACT

In this paper, we examine the electrical power-generation potential of a domestic-scale solar combined heating and power (S-CHP) system featuring an organic Rankine cycle (ORC) engine and a 15-m^2 non-concentrated solar-thermal collector array. The system is simulated with a range of organic working fluids and its performance is optimised for operation in the UK climate. The findings are applicable to similar geographical locations with significant cloud coverage, a low solar resource and limited installation areas. A key feature of the system's design is the implementation of fixed fluid flow-rates during operation in order to avoid penalties in the performance of components suffered at part-load. Steady operation under varying solar irradiance conditions is provided by way of a working-fluid buffer vessel at the evaporator outlet, which is maintained at the evaporation temperature and pressure of the ORC. By incorporating a two-stage solar collector/evaporator configuration, a maximum net annual electrical work output of 1070 kW h yr^{-1} (continuous average power of 122 W) and a solar-to-electrical efficiency of 6.3% is reported with HFC-245ca as the working fluid at an optimal evaporation saturation temperature of 126 °C (corresponding to an evaporation pressure of 16.2 bar). This is equivalent to ~32% of the electricity demand of a typical/average UK home, and represents an improvement of more than 50% over a recent effort by the same authors based on an earlier S-CHP system configuration and HFC-245fa as the working fluid [1], thus highlighting the gains possible when using optimal system configurations and fluids and suggesting that significant further improvements may be possible. A performance and simple cost comparison with stand-alone, side-by-side PV and solar-thermal heating systems is presented.

1. Introduction

Solar energy has the potential to meet a significant proportion of household demands for heating and electricity in the UK, despite its comparatively low annual yield of incident solar radiation (~1000 kW h m^{-2} yr^{-1} for southern UK compared to ~1800 kW h m^{-2} yr^{-1} for parts of southern Europe) [2]. Distributed domestic solar-power provision is conventionally a choice of either electricity generation via photovoltaic (PV) devices, or water heating via solar-thermal collectors. The feasibility of installing these as side-by-side systems for provision of both heating and power is limited by cost and space availability. At present, the only available technologies that can provide both heating and power from the same area of solar collector array are hybrid PV-thermal (PVT) systems, which are expensive and have a limited ability to meet time-varying demand ratios for heating and power [3–5].

* Corresponding author.
E-mail address: c.markides@imperial.ac.uk (C.N. Markides).

http://dx.doi.org/10.1016/j.apenergy.2016.04.041
0306-2619/

Nomenclature

Symbols

A	area, m^2
c_1	collector heat loss coefficient, $W/(m^2\,K)$
c_2	temperature dependence of the heat loss coefficient, $W/(m^2\,K^2)$
c_3	wind speed dependence of the heat loss coefficient, $J/(m^3\,K)$
c_4	sky temperature dependence of the heat loss coefficient, $W/(m^2\,K)$
c_5	solar collector effective thermal capacity, $J/(m^2\,K)$
c_6	wind-dependence of the collector optical (zero-loss) efficiency, s/m
h	specific enthalpy, J/kg
h_c	convective heat transfer coefficient, $W/(m^2\,K)$
F'	collector efficiency factor, –
G	solar irradiance, W/m^2
K_θ	solar collector incident angle modifier, –
$\dot{m}$	mass flow-rate, kg/s
P	pressure, bar
s	specific entropy, J/kg
T	temperature, K
t	time, s
U	overall heat transfer coefficient, $W/(m^2\,K)$
W	work, W
X	exergy, J
x	vapour quality, –
ε	heat exchanger effectiveness parameter, –
η	efficiency, –
η_0	solar collector optical (zero-loss) efficiency, –
$(\tau\alpha)$	effective transmittance-absorptance product, –

Subscripts

a	ambient air
cr	critical
bv	working fluid buffer vessel
bubble	bubble-point (saturated liquid condition)
exp	expander
gen	electricity generation
i, o	inner, outer
in, out	inlet, outlet
liq	liquid
n	normal incidence
r	regenerator
s	isentropic process
sat	saturation
sc	solar collector
sf	solar circulating fluid
wf	ORC working fluid
1,2,3,...	cycle state points

An alternative to PV-based technologies for electrical power generation from solar energy are solar-thermal technologies that convert heat to power via a suitable thermodynamic (heat) engine. Organic Rankine cycle (ORC) systems are one such technology that has been of recent considerable interest for low-grade heat conversion to useful power, including in waste-heat and renewable (i.e. solar, geothermal) energy research [6]. An attractive feature of solar-ORC systems is their ability to operate efficiently and affordably at lower temperatures and on smaller scales than solar-power systems based on steam-Rankine cycle technology. This opens up the possibility of developing the technology for geographical regions with a low solar resource and for distributed-level applications [7]. Despite this, a significant amount of experimental and modelling research on these systems have focused on application to regions with abundant solar resource and collector array areas beyond the size of what could be easily accommodated on the roof of a domestic property. Quoilin et al., [8] described a 3 kW_e ORC system for electricity-generation in a rural, off-grid community in Lesotho, southern Africa. The system was indirectly heated by a 75-m^2 concentrating parabolic trough collector (PTC) array with an automated tracking system and also included a 2-m^3 quartzite packed bed thermal store, while the power block featured a two-stage scroll expander configuration. Manolakos et al., [9] designed and tested an ORC reverse osmosis (RO) desalination system in Athens, Greece, indirectly heated by an evacuated tube solar collector array of gross area 216 m^2. The system incorporated a 2.5 kW reverse-operated scroll compressor as the expansion device, and was connected to the RO system via a belt and pulley arrangement. Wang et al., [10] investigated the performance of a 1.73 kW_e experimental ORC system in Tianjin, China, featuring a rolling-piston expander and powered by a 24 m^2 array of flat-plate collectors and a 20 m^2 array of evacuated tube collectors arranged in a parallel configuration. A key feature of this system was that the working fluid was directly evaporated in the solar collectors.

An important design-challenge for the successful operation of solar-thermal power systems is the ability to deal with time-varying incident radiation intensity. Thermal energy storage (TES) solutions can provide buffering for stable operation on a timescale of minutes (using small fluid buffer vessels) to hours (using large tanks of molten salts or packed beds of solid materials). Casati et al. [11] presented a range of a TES concepts for use in solar ORC systems. The authors noted that the ability to use working fluids with a "dry" (positive-gradient) vapour-saturation curve in these systems was highly favourable for solutions that consider thermal storage via direct storage of the working fluid. If the working fluid is stored under pressure as a saturated liquid, vapour can be generated by allowing the fluid to expand isenthalpically (known as flashing), and then fed to the expander. For very dry fluids, expansion from a saturated liquid to a saturated or superheated vapour state can be achieved with a relatively small drop in pressure. Working fluid storage for steam generation been used historically for various process applications. Steinmann and Eck [12] reviewed a number of configurations for steam accumulators as TES in steam-Rankine concentrating solar power (CSP) plants. A noted limitation of basic *sliding-pressure* steam accumulators in which the water working fluid is stored in two-phase (liquid–vapour) thermodynamic equilibrium is the associated drop in pressure of fluid in the vessel as steam is discharged. The aforementioned authors presented a concept for *constant-pressure* storage using encapsulated phase change materials (PCM). PCMs make use of solid–liquid phase change in order to achieve high energy storage densities ($\sim$100 kW h m^{-3}, compared to $\sim$ 10 kW h m^{-3} for sensible liquid storage) under isothermal conditions. Thus temperature (and hence pressure) of the saturated steam or vapour supply can be maintained. This concept has been recently employed with success in prototype steam generator systems [13], and has been proposed for use in a refrigerant-based solar-ORC system by Jing et al., [14]. Other energy storage solutions considered for use in solar-thermal systems are thermo-chemical

Please cite this article in press as: Freeman J et al. Working fluid selection and electrical performance optimisation of a domestic solar-ORC combined heat and power system for year-round operation in the UK. Appl Energy (2016), http://dx.doi.org/10.1016/j.apenergy.2016.04.041

storage technologies that make use of either sorption processes or reversible chemical reactions such as hydration or carbonation of metal oxides. At present, solar applications of thermo-chemical storage have predominantly been of the sorption-storage type when working with charging temperatures $\leqslant$150 °C, and deliver reported energy densities of 100–600 kW h/m^3. Chemical-reaction energy storage meanwhile typically tends to be considered in higher temperature applications where charging temperatures $\geqslant$400 °C can be achieved [15–18].

The aim of this paper is to assess the electricity generating potential of an ORC-based solar combined heating and power (S-CHP) system when operating at lower solar irradiance levels and smaller scales. The UK is a region of highly variable solar irradiance quality, both spatially and temporally. Annual average irradiance varies from 128.4 W m^{-2} in southern England to 71.8 W m^{-2} in northern Scotland [19]. In London, typically 60% of the annual insolation received is diffuse [2], and therefore largely unusable by concentrating collectors that use reflecting surfaces to focus incoming radiation onto a smaller central receiver. Advances in non-concentrating solar-thermal technology have resulted in collectors with an improved ability to absorb solar radiation with high efficiency and minimal thermal losses to the environment through convection and re-radiation. Evacuated-tube collectors (ETC) use a vacuum envelope to suppress convection and therefore are able to operate with higher absorber temperatures and in colder ambient air conditions than most flat-plate collectors (FPC). However due to their cylindrical shape, required for structural stability in the presence of a vacuum, the gross area efficiency of installed ETC modules is significantly limited. In recent years numerous companies and research institutions (TVP Solar, SRB Energy, Genersys, CERN) have developed or patented manufacturing techniques for evacuated flat-plate collectors (EFPC), combining efficient high-temperature operation with a high gross area utilisation. Furthermore, these collectors have been developed specifically to target process-heat applications such as steam generation, desalination, absorption refrigeration and power generation at temperatures in the range 100–300 °C [20–22].

The economic case for domestic solar and other renewables technologies is based not only their ability to displace primary energy from fossil fuels. The 8.6 GW incease in installed capcity of PV in the UK has coincided with the introduction of the Feed-in Tariff (FIT) scheme [23]. At the time of writing, the UK offers an FIT payment rate of 4.39 p kW h$_e^{-1}$ for electrical energy generated from PV[1], and also a Renewable Heat Incentive (RHI) tariff of 19.51 p kW h$_{th}^{-1}$ for thermal energy generated by domestic solar hot water systems [24]. There is, however, no specific incentive scheme for domestic solar thermal technologies that also produce an electrical output; and the rapid decrease in the PV generation FIT payment from 43.3 p kW h$_e^{-1}$ in 2011, to 12.03 p kW h$_e^{-1}$ in 2015, to its present value in 2016, make payback period comparisons of such technologies with PV based on incentivisation schemes difficult and susceptible to change.

In an earlier work, the authors presented a system model of a domestic-scale S-CHP system and simulated its performance in the UK climate [1]. The system model featured a solar collector array, a basic four-component (*non-regenerative*) ORC engine and a hot-water cylinder. Both the ORC engine and the hot-water cylinder received a thermal energy input from the solar collector array to meet a variable demand for heating and power. The ORC working fluid was the hydrofluorocarbon (HFC) refrigerant R245fa, also investigated for use in the aforementioned solar-ORC systems by Quoilin et al. [8] and Wang et al. [10]; and chosen for its low toxicity, flammability and ozone depletion potential (ODP), and also its low saturation temperature at atmospheric pressure. The system's fixed flow-rates and fixed operating temperatures and pressures were selected for maximum work production on an "annual-average" day and then simulated over an annual period. It was found that the total electrical work output was 700 kW h yr^{-1} (80 W average), and that the whole system capital cost was between £4400–5500. However, the system was only crudely optimised and several potential areas for performance enhancement were identified. In this paper, a wider range of working fluids will be considered in order to find the optimum fluid to maximise annual work output from the system in the UK setting. The performance of a given working fluid is dependent upon the evaporation temperature of the Rankine cycle, which is itself dependent upon the choice of solar-thermal collector design and the solar irradiance characteristics of the chosen location. Consideration will also be given to system configurations that enable efficient operation of the solar collector array and continuous power output under intermittent solar irradiance conditions.

2. Modelling methodology

2.1. System model description

A schematic diagram of the investigated S-CHP system is shown in Fig. 1a. Pump 1 is used to pressurise the working fluid from a saturated liquid at State 1 to its evaporation pressure at State 2a. The fluid is then preheated to State 2b in the regenerator heat-exchanger, before mixing with the saturated liquid stream from the buffer vessel circulated by Pump 2. The combined fluid-stream at State 2c enters the evaporator where it is heated by the solar-collector fluid circulated by Pump 3. Fluid leaving the evaporator at State 3a then proceeds to the buffer vessel. The buffer vessel is assumed to be held at a constant temperature equal to the evaporation temperature of the ORC, such that working fluid may be stored in a two-phase state within. A similar concept was proposed earlier, in the work by Jing et al. [14], where it was suggested that the buffer vessel temperature could be maintained by conduits filled with phase change material (PCM). Various other concepts for the use of the working fluid itself as the thermal storage medium in solar steam-Rankine and ORC plants have been investigated by previous authors [12,11], and a preliminary attempt is made in the present work to consider this aspect of the system design and implementation in terms of the storage need in this particular application. Saturated liquid from the buffer vessel is recycled to the evaporator by Pump 2, while saturated vapour from the buffer vessel (State 3b) proceeds to the expander where it is expanded to the condensation pressure, thus producing shaft work. Low pressure vapour is exhausted from the expander (State 4a) and cooled (de-superheated) in the regenerator (State 4b) before being returned to the initial saturated liquid condition (State 1) in the condenser.

The benefits of the system configuration described above are as follows: (1) the buffer vessel suppresses the variations in the expander inlet vapour quality due to the intermittency of the solar heat-source, so that periods of steady operation can be maintained for longer than for a system with no thermal/fluid store; (2) the design enables system operation with fixed flow-rates so that the pumps, expander and heat exchangers can operate at their design points; (3) the design enables a steady fluid temperature to be achieved at the evaporator outlet, which simplifies the task of identifying the optimal working fluid and evaporation temperature/pressure over the annual period in the chosen climate; (4) the active real-time operational control strategy for system, also in response to changing loads/demands, is greatly simplified.

[1] As of 8 February 2016, and applicable to systems <4 kW$_e$ installed on dwellings with the highest Energy Performance Certificate (HPC) rating

Please cite this article in press as: Freeman J et al. Working fluid selection and electrical performance optimisation of a domestic solar-ORC combined heat and power system for year-round operation in the UK. Appl Energy (2016), http://dx.doi.org/10.1016/j.apenergy.2016.04.041

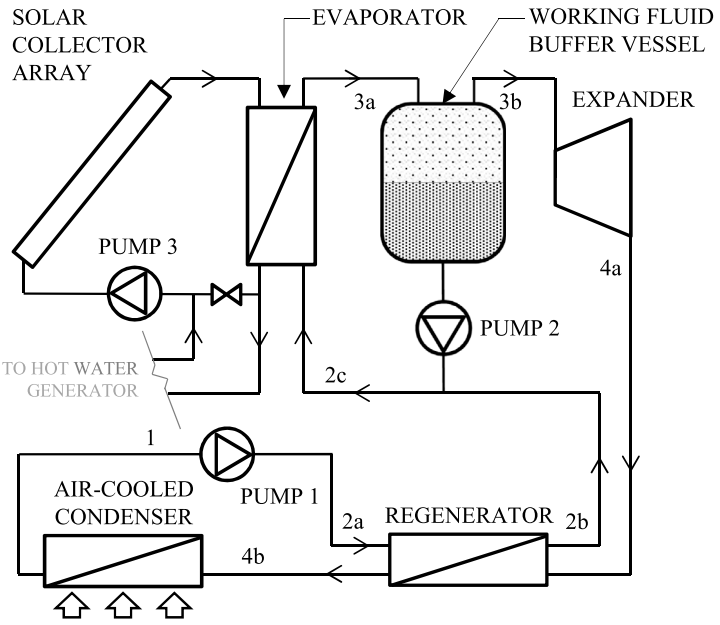

(a) Schematic diagram of the S-CHP system with a single-stage solar collector array.

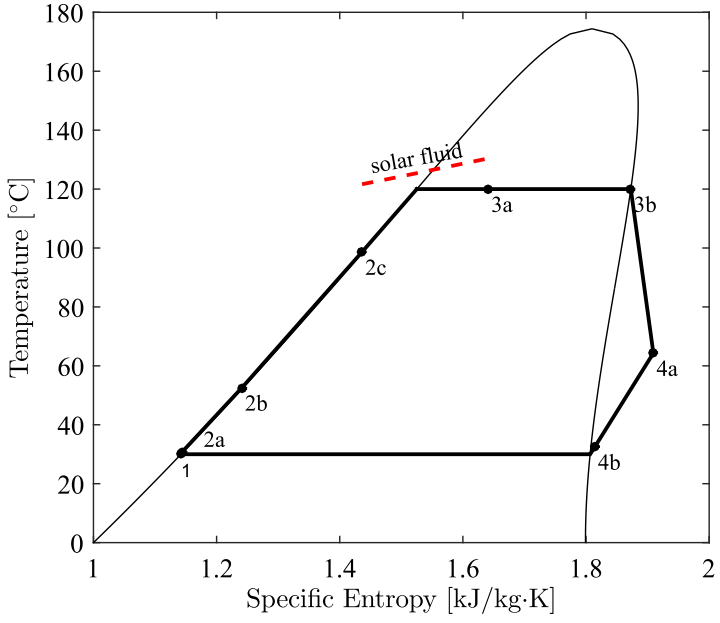

(b) Temperature-entropy (T-s) diagram of the ORC with R245ca as the working fluid.

Fig. 1. Single-stage collector array S-CHP system configuration and ORC thermodynamic cycle diagram.

A variant of the aforementioned system will also be examined that incorporates a two-stage solar collector array, based on the configuration proposed by Jing et al. [14]. In the modified configuration, shown in Fig. 2, the ORC working fluid heat addition process is split into separate sensible and latent stages, each served by separate heat exchangers and dedicated sections of the solar collector array (although the total collector array area remains the same as for the single-stage configuration). The sensible pre-heating stage occurs prior to mixing with the recirculated flow from the buffer vessel, and thus the two streams are closer together in temperature before mixing which is thermodynamically (i.e., exergetically) preferable. Furthermore, the lower average temperature of the solar collector circulating fluid in the first stage allows for a closer match in temperature between the fluid streams (illustrated by the lines labelled "Stage 1" and "Stage 2" in Fig. 2b), and a higher overall solar collector array efficiency. This two-stage configuration requires the inclusion of an additional pump and heat exchanger compared to the single-stage configuration presented above, the cost impact of which are discussed briefly in Section 3.2.

2.2. Solar-thermal collector equations

The model of solar-thermal collector chosen for this study is the TVP SOLAR *HT-Power*, a high efficiency evacuated flat-plate collector highlighted for its potential in ORC applications in the study by Calise et al. [25]. The properties of the solar collector are listed in Table 1. In the aforementioned study, the diathermic oil DOWTHERM A [26] is chosen as an appropriate circulating fluid for this

Please cite this article in press as: Freeman J et al. Working fluid selection and electrical performance optimisation of a domestic solar-ORC combined heat and power system for year-round operation in the UK. Appl Energy (2016), http://dx.doi.org/10.1016/j.apenergy.2016.04.041

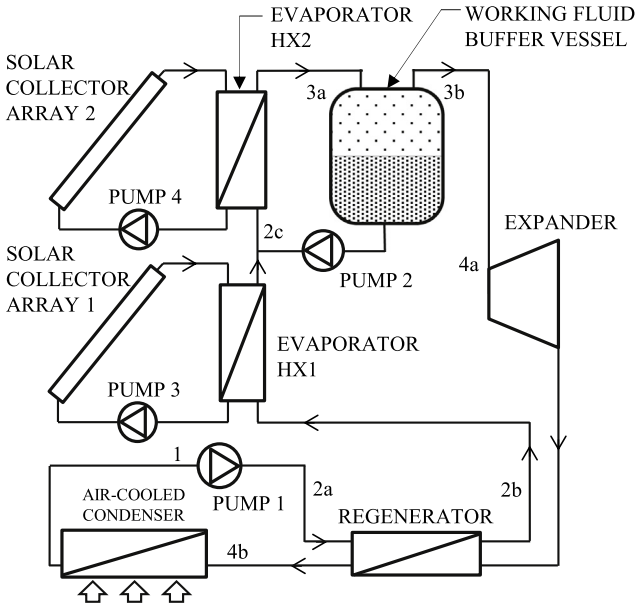

(a) Schematic diagram of the S-CHP system with a two-stage solar collector array.

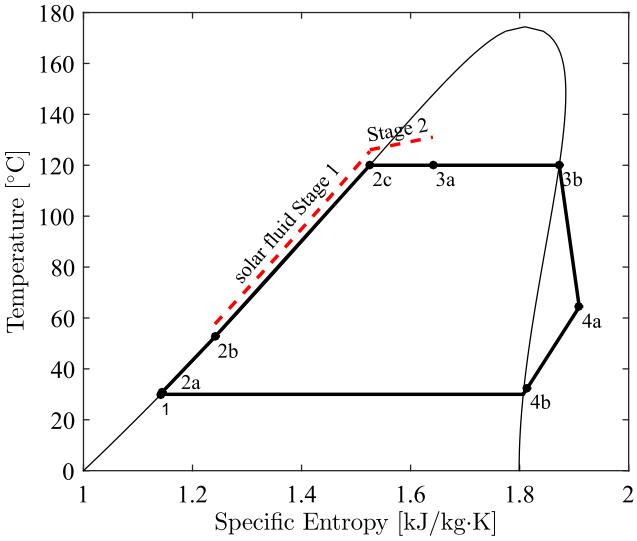

(b) Temperature-entropy (T-s) diagram of the ORC with R245ca as the working fluid.

Fig. 2. Two-stage collector array S-CHP system configuration and ORC thermodynamic cycle diagram.

Table 1
Solar-ORC S-CHP system model parameters used in the present study.

Solar collector parameters[a]		ORC parameters	
η_0	0.82	η_{pump}, η_{exp}	0.65, 0.75
c_1, c_2	0.399, 0.0067	η_{gen}	0.90
$K_{\theta,(\theta=50^\circ)}$	0.91	ε_r	0.95
ΔP_{sc}[b](kPa)	0.7	T_{cond}[c] (°C)	30

[a] Information taken from *HT-Power* product datasheet [20] and Calise et al. [24].
[b] Corresponding to $\dot{V}_{ref} = 51\ \mathrm{L\,m^{-2}\,hr^{-1}}$.
[c] If $T_{sat}(P_{atm}) > 30\ ^\circ\mathrm{C}$, then $T_{cond} = T_{sat}(P_{atm})$.

solar collector due to its temperature application range, and therefore the same fluid will be used for the simulations in the present work. The useful energy output from the solar collector can be predicted as a function of the local climatic conditions using the widely-adopted model by Perers and Bales [27]:

$$\dot{Q}_{sf} = F'(\tau\alpha)_n K_{\theta,b} G_b + F'(\tau\alpha)_n K_{\theta,d} G_d - c_6 u_w G - c_1(\overline{T}_{sc} - T_a) - c_2(\overline{T}_{sc} - T_a)^2 - c_3 u_w(\overline{T}_{sc} - T_a) + c_4\left(E_L - \sigma T_a^4\right) - c_5 \frac{d\overline{T}_{sc}}{dt}. \quad (1)$$

In line with similar previous efforts in the literature, the evacuated flat-plate collector in the present work will be modelled according to the following assumptions: (i) the wind-speed and long-wave irradiance dependent terms for high-efficiency glazed collectors are less significant than for low-efficiency unglazed collectors and therefore may be neglected, as is the standard approach for evacuated collectors [27,28,14,29]; (ii) the response time of the collector is small compared to the hourly time-interval for the climate data used in the simulation [30]; (iii) the value for the diffuse radiation incidence angle modifier is close to 1 for all angles of incidence [31]. This allows the associated terms in Eq. (1) to be omitted, resulting in the following expression for the collector thermal efficiency:

Please cite this article in press as: Freeman J et al. Working fluid selection and electrical performance optimisation of a domestic solar-ORC combined heat and power system for year-round operation in the UK. Appl Energy (2016), http://dx.doi.org/10.1016/j.apenergy.2016.04.041

$$\eta_{sc} = \eta_0 K_\theta - c_1 \frac{(\overline{T}_{sc} - T_a)}{G} - c_2 \frac{(\overline{T}_{sc} - T_a)^2}{G}, \quad (2)$$

where $K_\theta = (K_{\theta,b} G_b + G_d)/(G_b + G_d)$. For the calculation of the overall solar collector array efficiency, a modified expression is required that takes into account the non-linear decrease in collector efficiency with fluid temperature. Thus Jing et al. [14] derive the following expression for the collector array efficiency by integrating the local collector efficiency over the total length of the array, provided that the inlet and outlet solar fluid temperatures ($T_{sf,in}, T_{sf,out}$) are known:

$$\eta_{sc,array} = \frac{(c_2/G)(\varphi_2 - \varphi_1)\left[c_{p,0}(T_{sf,out} - T_{sf,in}) + 0.5\alpha(T_{sf,out} - T_{sf,in})(T_{sf,out} + T_{sf,in} - 2T_{sf,0})\right]}{\left[c_{p,0} + \alpha(T_a - T_{sf,0} + \varphi_1)\right] \ln\left(\frac{T_{sf,out} - T_a - \varphi_1}{T_{sf,in} - T_a - \varphi_1}\right) + \left[c_{p,0} + \alpha(T_a - T_{sf,0} + \varphi_2)\right] \ln\left(\frac{\varphi_2 - T_{sf,in} + T_a}{\varphi_1 - T_{sf,out} + T_a}\right)}, \quad (3)$$

where $c_{p,0}, \alpha$ and T_0 are parameters that describe a linear variation of specific heat capacity with temperature for the solar heat-transfer fluid such that $c_{p,sc} = c_{p,0} + \alpha(T_a - T_{sf,0})$, and parameters φ_1 and φ_2 are the solution values (negative and positive, respectively) of the quadratic function $\eta_0 K_\theta - c_1\varphi/G - c_2\varphi^2/G = 0$. By assuming that the quantity of solar radiation absorbed by the collector array is equal to the enthalpy rise of the heat-transfer fluid:

$$\dot{Q}_{sf} = \eta_{sc} A_{sc} G = (\dot{m} c_p)_{sf} (T_{sc,out} - T_{sc,in}). \quad (4)$$

Finally, in order to calculate the pumping power required to circulate the solar fluid, pressure drops in the solar collector array are estimated using data provided by the manufacturer (see Table 1).

2.3. Heat exchanger equations

A finite element method is used to model the heat transfer process in the evaporator. The evaporator is modelled as a counterflow concentric-tube heat exchanger, with the ORC working fluid flowing inside the tube and the solar heat-transfer fluid flowing in the annulus. The heat exchanger length is divided into N finite elements, and the enthalpy and temperatures of the ORC working fluid and solar collector heat-transfer fluid for the $(n+1)$th element are calculated from:

$$h_{wf,n+1} = h_{wf,n} + \frac{U\pi D_i N_{tubes}(T_{sf,n} - T_{wf,n})}{\dot{m}_{wf}} \Delta L, \quad (5)$$

$$T_{sf,n+1} = T_{sf,n} + \frac{U\pi D_i N_{tubes}(T_{sf,n} - T_{wf,n})}{(\dot{m} c_p)_{sf}} \Delta L, \quad (6)$$

where the total heat transfer coefficient between the fluid streams is $U = 1/(h_{c,i}^{-1} + h_{c,o}^{-1})$. Note that due to the counterflow arrangement of the heat exchanger, element $n = 1$ of the heat exchanger represents the working fluid inlet and the solar fluid outlet. The evaporator heat exchangers are approximately sized so that the "pinch-point" temperature difference between the fluid streams is $\Delta T_{pinch} \approx 5$ K. The heat exchangers are sized with a suitable number of parallel tubes to achieve $Re \approx 3000$ in the solar fluid stream. For heat transfer between the pipe wall and the ORC working fluid in the liquid phase, the local heat transfer coefficients are calculated using Nusselt number correlations given in Incropera et al. [32]. For heat transfer between the pipe wall and the working fluid in the two-phase region, the local heat transfer coefficients are calculated using the Lockhart-Martinelli parameter approach described in Wang and Touber [33]. With both fluid flow rates and the working fluid evaporator inlet temperature supplied as input parameters, the working fluid outlet and solar fluid inlet and outlet temperatures are solved so that $(\dot{m}\Delta h)_{wf} = -(\dot{m}\Delta h)_{sf}$. Finally, the pressure drops in the evaporator heat exchangers are calculated using the Reynolds number/friction factor correlations in Incropera et al. [32].

2.4. ORC equations

The power consumed by the ORC pump and the (gross) power output of the ORC expander are both calculated using their respective isentropic efficiencies (see Table 1):

$$\dot{W}_{pump1} = \frac{1}{\eta_{pump}} \cdot \dot{m}_{pump1}(h_{2a} - h_1), \quad (7)$$

$$\dot{W}_{exp} = \eta_{exp} \dot{m}_{pump1}(h_{3b} - h_{4a,s}), \quad (8)$$

where h_1 is the specific enthalpy of the working fluid as a saturated liquid at the condensation pressure, and h_{3b} is the specific enthalpy of the working fluid as a saturated vapour at the evaporation pressure.

The pump and expander isentropic efficiency values are reported in Table 1, where η_{exp} is chosen to be broadly representative of a generalised small-scale positive-displacement expander, and is within the range of values reported in various experimental studies on such machines [34–41]. Similarly, the value of η_{pump} is within the range of those used in similar modelling studies [42,35,43,44]. It is noted that the eventual performance prediction of the solar-ORC S-CHP system will be significantly more sensitive to the former. It will be shown later that the pump consumed power is of the order of 4% of the expander gross generated power, or ~1:25. If the isentropic efficiency of the pump is varied by a factor of two, e.g., representing a deviation of the factor of two between the current model and actual pump performance, the corresponding deviations (errors) in the efficiency and power output estimations of the model will only amount to 4%.

The net electrical power output from the ORC system is:

$$\dot{W}_{net} = \eta_{gen}\dot{W}_{exp} - \dot{W}_{pump1} - \dot{W}_{pump2} - \dot{W}_{pumps3\&4}. \quad (9)$$

The change in enthalpy of the working fluid in the regenerator heat exchanger is calculated using an effectiveness parameter ε_r:

$$h_{2b} = h_{2a} + \varepsilon_r(h_{4a} - h_{4b'}), \quad (10)$$

where $h_{4b'}$ is the specific enthalpy of the working fluid at the condensation pressure and at the temperature $h_{4b'} = T_{2a}$.

2.5. Fluid flow-rates

Increasing the flow-rate of Pump 2 relative to Pump 1 allows for a closer match between the hot and cold fluid temperatures in the evaporator, a higher mass flow-rate and hence better heat transfer coefficient in the hot fluid and a more uniform fluid temperature in the solar collector array at the expense of a larger pumping power requirement. A mass flow-rate ratio of 1:2 for Pumps 1 and 2 is found to offer a good compromise, such that $\dot{m}_{pump2} = 2 \cdot \dot{m}_{pump1}$. The solar heat transfer-fluid flow-rate circulated by Pump 3 is set for a temperature glide of $\Delta T_{sf} = 5$ K between the solar fluid inlet

Please cite this article in press as: Freeman J et al. Working fluid selection and electrical performance optimisation of a domestic solar-ORC combined heat and power system for year-round operation in the UK. Appl Energy (2016), http://dx.doi.org/10.1016/j.apenergy.2016.04.041

and the pinch point corresponding to the working fluid bubble point, for a design condition in which the vapour quality at the evaporator outlet $x_{3a} = 0.33$. Thus:

$$\dot{m}_{\text{pump3}} = \frac{(\dot{m}_{\text{pump1}} + \dot{m}_{\text{pump2}})(h_{3a} - h_{\text{bubble}})}{c_{\text{p,sf}}\Delta T_{\text{sf}}}. \quad (11)$$

For the two-stage collector configuration, the mass flow-rate circulated by Pump 4 is sized by a similar method as above to achieve an approximately parallel temperature glide between two fluid streams in the first stage heat exchanger, as shown in Fig. 2b.

2.6. Working fluid buffer vessel

As mentioned earlier in Section 2.1, the presence of the buffer vessel at the evaporator outlet ensures that the working fluid always enters the expander as a saturated vapour at the chosen cycle evaporation temperature. Heat transfer in the buffer vessel is not treated in detail in this work. Following the approach of Jing et al. [14], the buffer vessel is assumed to be perfectly insulated, zero-dimensional and of sufficient size to provide the required buffering for steady performance of the system over the entire annual period. Thus for each time-step of the annual simulation, the change in internal energy of the total fluid mass in the buffer vessel is:

$$\Delta U_{\text{bv}} = \left[(\dot{m}_{\text{pump1}} + \dot{m}_{\text{pump2}})h_{3a} - \dot{m}_{\text{pump1}}h_{3b} - \dot{m}_{\text{pump2}}h_{\text{bubble}}\right]\Delta t. \quad (12)$$

The size of the buffer vessel is not provided as an input to the calculations, but the variation in internal energy required to maintain the steady outlet condition to the expander for the the duration of the simulation period is reported as an output of the calculations, and will form the basis of discussion for TES options in Section 3.3.

2.7. Second law analysis

A second law (exergy) analysis will be used to evaluate the maximum convertible work from the hot fluid stream leaving the solar collector array in order to determine the exergy efficiency of the S-CHP system in power generation mode. In an earlier work by the authors, a method was outlined for evaluating the maximum convertible work from a range of solar collectors operating at their optimum outlet temperature and mass flow-rate [45]. The flow-rate of exergy in the fluid stream leaving the collector is calculated as the integral of the power produced by an infinite number of infinitesimal Carnot engines operating between the hot stream and the cold reservoir. For this analysis, it will be assumed that the cold reservoir is the ambient air, and that the ideal energy conversion process results in the fluid stream being cooled to the ambient air temperature before it is returned to the collector inlet. Thus, the collector outlet temperature $T_{\text{sc,out}}$ is varied by adjusting the mass flow-rate of the solar fluid and the maximum work is evaluated. The resulting expression is as follows:

$$\dot{X}_{\text{sc,out}} = \eta_{\text{sc}}A_{\text{sc}}G\left[1 - \left(\frac{T_{\text{sc,out}}}{T_{\text{a}}} - 1\right)^{-1}\ln\left(\frac{T_{\text{sc,out}}}{T_{\text{a}}}\right)\right]. \quad (13)$$

The analysis in the present work is concerned with the relative improvements in exergy efficiency as a result of the optimisation of the system operating parameters. Thus, the reference value for the exergy efficiency calculation is taken here as the maximum exergy flow in the fluid stream leaving the collector (corresponding to the optimum collector flow-rate and temperature), rather than the exergy flow associated with the solar irradiance incident on the collector surface. Exergy losses associated with the collector design and materials selection (e.g. the transmittance-absorptance properties of the glazing and absorber) are not included in this analysis. Together, these collector-associated losses account for approximately 90% of the exergy destruction in the entire system, as noted in our earlier work [1].

2.8. Annual simulation

For the annual assessment, the system performance is evaluated using London, UK annual climate data (latitude: 51.15°, longitude: −0.18°) comprised of hourly solar irradiance and air temperature values [46]. The calculations are performed in MATLAB using an implicit numerical method with an hourly time-step. An optimal tilt angle is chosen for the solar collector array in order to maximise the annual solar irradiation received (the optimal tilt angle calculated using the climate dataset is found to be 40.5° for a due south orientation). The ORC system is operational during all hours in which the climatic conditions (solar irradiance and ambient air temperature) are sufficient such that $\eta_{\text{sc}} > 0$. During these hours, the ORC expander operates under constant flow-rate and power-output conditions. If $h_{3a} > h_{x=0.33}$, then heat (enthalpy) is stored in the buffer vessel while if $h_{3a} < h_{x=0.33}$ then heat (enthalpy) is released from the buffer vessel. The area of the solar collector array is fixed at $A_{\text{sc}} = 15\ \text{m}^2$ [1] and the fixed value for the mass flow-rate of Pump 1 is solved so that the net annual internal energy gain by the buffer vessel is zero ($\sum_{hr=1}^{8760}\Delta U_{\text{bv}} = 0$). This procedure is repeated for each working fluid over the range of evaporation temperatures. The overall efficiency of the system operating over the annual period is evaluated as follows:

$$\eta_{\text{overall}} = \frac{\sum_{hr=1}^{8760}\dot{W}_{\text{net}}}{\sum_{hr=1}^{8760}GA_{\text{sc}}}. \quad (14)$$

The annual exergy efficiency of the system is evaluated as the net annual work output from the ORC engine divided by maximum convertible work (or exergy) output from the solar collector array operating at its optimum temperature and flow-rate at each time-instant:

$$\eta_{\text{exergy}} = \frac{\sum_{hr=1}^{8760}\dot{W}_{\text{net}}}{\sum_{hr=1}^{8760}\dot{X}_{\text{sc,out,max}}}. \quad (15)$$

3. Results and discussion

3.1. Comparison of working fluids under steady-state conditions for a single-stage collector system

In order to understand how the optimum choice of working fluid and evaporation temperature/pressure varies with solar irradiance, the single-stage system is simulated firstly under steady-state conditions. A range of hydrocarbon (HC), hydrofluorocarbon (HFC), hydrochlorfluorocarbon (HCFC) and chlorofluorocarbon (CFC) refrigerants are chosen that have been investigated in previous works on low temperature and solar ORC systems [47–49]. Only pure fluids are considered here, although working-fluid mixtures have been shown to offer improved thermodynamic efficiency due to non-isothermal phase change at constant pressure and hence reduced temperature differences and higher average temperatures of heat addition in ORC systems [50,51]. While mixtures are of interest for future work, such an evaluation is beyond the scope of the present study. Furthermore, the consideration of complex phenomena such as reduced heat transfer coefficients for mixtures compared to their pure fluid counterparts is of importance when evaluating the overall impact on system efficiency and cost [52].

Please cite this article in press as: Freeman J et al. Working fluid selection and electrical performance optimisation of a domestic solar-ORC combined heat and power system for year-round operation in the UK. Appl Energy (2016), http://dx.doi.org/10.1016/j.apenergy.2016.04.041

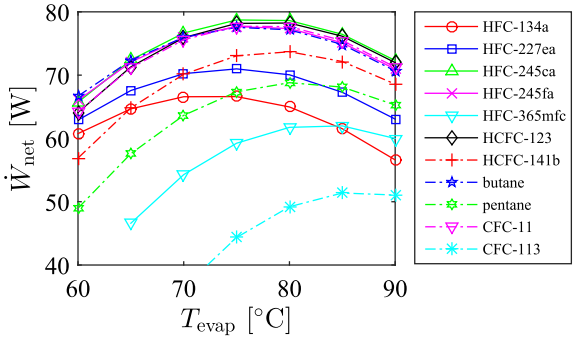

(a) Low solar irradiance ($G = 150\ \mathrm{W\,m^{-2}}$).

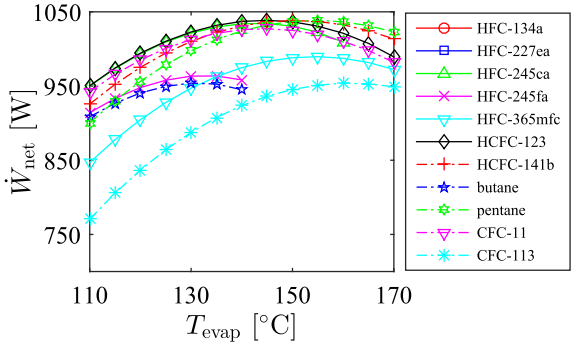

(b) High solar irradiance ($G = 800\ \mathrm{W\,m^{-2}}$).

Fig. 3. ORC net power output as a function of the evaporation temperature (saturation pressure) for conditions: (a) $G = 150\ \mathrm{W\,m^{-2}}$ and $T_a = 20\ °C$; and (b) $G = 800\ \mathrm{W\,m^{-2}}$ and $T_a = 20\ °C$.

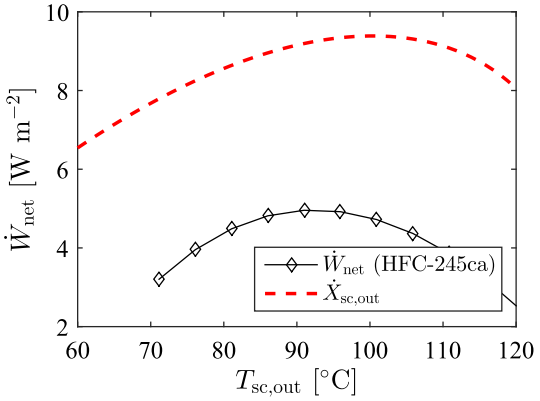

(a) Low solar irradiance ($G = 150\ \mathrm{W\,m^{-2}}$).

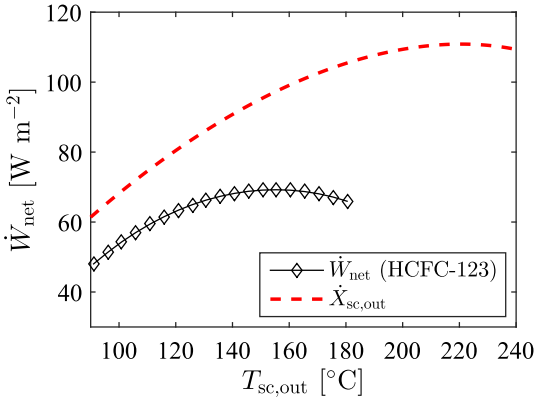

(b) High solar irradiance ($G = 800\ \mathrm{W\,m^{-2}}$).

Fig. 4. ORC net power output as a function of the solar collector array outlet temperature for: (a) $G = 150\ \mathrm{W\,m^{-2}}$ and $T_a = 20\ °C$; and (b) $G = 800\ \mathrm{W\,m^{-2}}$ and $T_a = 20\ °C$. Also shown is the solar collector exergy output (upper limit dashed line) as a function of the mean collector temperature.

Fig. 3 shows the simulated power output from the system at a low irradiance level ($150\ \mathrm{W\,m^{-2}}$) and a high irradiance level ($800\ \mathrm{W\,m^{-2}}$), for the different working fluids considered herein and over a range of evaporation temperatures. For each irradiance level and working fluid the evaporation temperature is varied in finite increments and the system flow-rates are solved for a steady-state operation (corresponding to a vapour quality at State 3a of $x_{wf} = 0.33$, such that $\Delta U_{bv} = 0$). The resulting power output curves can then be used to identify the evaporation temperature that delivers maximum power output under steady-state irradiance conditions for each working fluid.

It can be observed in Fig. 3 that the highest net power outputs for both cases of low and high irradiance conditions are obtained with the fluids R245ca, R123 and R11. Furthermore, these fluids are found to perform well across a broad range of evaporation temperatures. The maximum net power output at the low irradiance level is 79 W (for working fluid R245ca), and is achieved at an ORC evaporation temperature of 78 °C. The maximum net power output at the high irradiance level is 1040 W (for working fluid R123) and is achieved at an ORC evaporation temperature of 144 °C. Fluids that perform well at low irradiance levels (corresponding to lower optimum evaporation temperatures) but poorly at high irradiance levels are R245fa and butane. Both of these fluids are limited by their low critical temperatures. Pentane and R141b, on the other hand, show the opposite characteristic, performing well at high irradiance levels but poorly at low irradiance levels compared to the other fluids. R113 and R365mfc perform less well at both low and high irradiance levels, and it should be noted that for these fluids the cycle condensation temperatures (48 °C and 41 °C respectively, corresponding to their saturation temperature at atmospheric pressure), are higher than for the other fluids considered here.

In Fig. 4 the net power-output from the ORC system per m^2 of solar collector array area is plotted and compared to the exergy output from the array as a function of the collector array outlet temperature (as given by Eq. (13)). At $G = 150\ \mathrm{W\,m^{-2}}$ it can be seen that the maximum exergy output from the collector array is $9.4\ \mathrm{W\,m^{-2}}$ (and corresponds to $T_{sc,out} = 101\ °C$), whereas the maximum net power output from the ORC system with the optimal working fluid and evaporation temperature combination is $5.3\ \mathrm{W\,m^{-2}}$, which corresponds to an exergy efficiency of 56%. At $G = 800\ \mathrm{W\,m^{-2}}$, the maximum exergy output from the collector array is $110\ \mathrm{W\,m^{-2}}$ (corresponding to $T_{sc,out} = 210\ °C$), whereas the maximum ORC net power output is $69.4\ \mathrm{W\,m^{-2}}$ at an exergy efficiency of 63%. As expected, the collector outlet temperature corresponding to maximum exergy is higher than that corresponding to the maximum net power from the ORC system in all cases. Further, it can also be observed by comparison with Table 2 that the temperature corresponding to maximum exergy for the high irradiance case is considerably higher than the critical temperature of all of the working fluids investigated. This suggests that the properties of the working fluids are imposing a limitation on the performance of the solar collector and the exergy efficiency of the system.

3.2. Comparison with a two-stage collector system

For the following analysis R245ca will be chosen as the ORC working fluid of interest due to its favourable performance, as identified in the previous section and its lower ODP compared to

Please cite this article in press as: Freeman J et al. Working fluid selection and electrical performance optimisation of a domestic solar-ORC combined heat and power system for year-round operation in the UK. Appl Energy (2016), http://dx.doi.org/10.1016/j.apenergy.2016.04.041

Table 2
Properties of candidate working fluids considered in the present study.

Fluid	ds/dT (J kg^{-1} K^{-1})	T_{cr} (°C)	P_{cr} (bar)	T_{sat}[a] (°C)	h_{fg}[b] (J kg^{-1})	$c_{p,liq}$[c] (J kg^{-1} K^{-1})	ODP[d]	GWP[e]
HFC-134a	-0.39	102	41	−26	155	1447	0	1300
HFC-227ea	0.76	102	29	−17	98	1198	0	3500
HFC-245ca	0.60	174	39	25	192	1387	0	726
HFC-245fa	0.19	154	37	15	177	1333	0	1050
HFC-365mfc	1.07	187	33	40	185	1387	0	794
Butane	1.03	152	38	−0.5	338	2470	0	4
Pentane	1.51	197	34	36	349	2339	0	3
HCFC-123	0.26	184	37	28	162	1026	0.02	0.02
HCFC-141b	0	204	42	32	215	1161	0.11	725
CFC-11	−0.13	198	44	24	172	886	1	4000
CFC-113	0.52	214	34	48	145	923	0.80	4800

[a] At $P_{atm} = 101.3$ kPa.
[b] At $T = 100$ °C.
[c] At $T = 30$ °C.
[d] Relative to R11.
[e] Relative to CO_2.

refrigerants R11 and R123. However, it should also be noted that, at least at present, R245ca is not widely available for purchase in bulk quantities in the UK.

The steady-state simulations are repeated for the two-stage collector array configuration and the results compared with those for the single-stage configuration. For each steady-state condition, the system flow-rates and the relative areas of the first and second-stage collector arrays are solved so that the ORC working fluid leaves the first heating stage as a saturated liquid and the second heating stage as a two-phase fluid at the target vapour quality of $x_{wf} = 0.33$ (illustrated by the *T-s* diagram in Fig. 2b). The results are compared to the single-stage configuration in Fig. 5.

For the two-stage configuration, the system is found to operate with a higher overall collector array efficiency, and the result is a 5% increase in maximum net power output in the low irradiance case and a 7% increase in maximum net power in the high irradiance case. It can also be observed that the peak power output for the two-stage configuration occurs at a higher evaporation temperature than for the single-stage configuration. This is most evident in the high irradiance case, for which the peak power output occurs at an evaporation temperature of 155 °C for the two-stage configuration compared to 144 °C for the single-stage configuration.

For the two-stage system the ratio of the first-stage collector array area to total collector array area (also shown in Fig. 5 on the right-hand *y*-axis) is found to increase with evaporation temperature. This can be easily understood by the increased ratio of sensible heating to latent heating of the Rankine cycle working fluid as evaporation temperature is increased. With the addition of the second stage heat exchanger, the overall heat transfer area increases by 42%. Taking this additional heat exchanger cost into account and also considering the need for the additional pump, the expected cost increase of the two-stage system relative to the single-stage system is in the region of €450-500. Thus the increase in system cost per additional Watt of nominal power output is approximately 6 €/W.

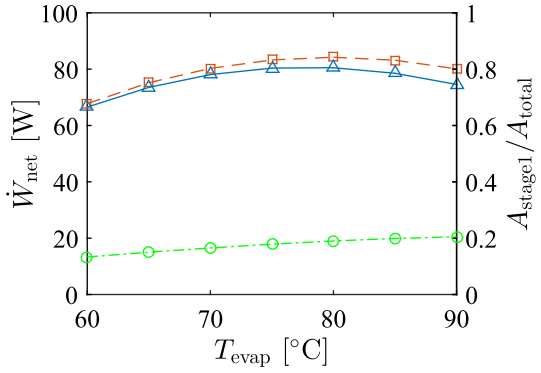

(a) Low solar irradiance ($G = 150$ W m^{-2}).

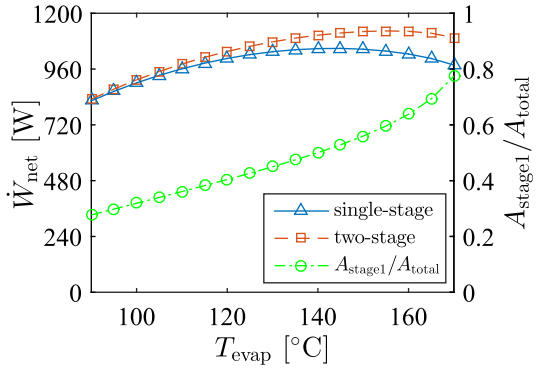

(b) High solar irradiance ($G = 800$ W m^{-2}).

Fig. 5. Comparison of the ORC net power output from single-stage and two-stage solar collector configurations (with the relative array areas of the two-stage configuration also shown), with R245ca as the working fluid and for conditions: (a) $G = 150$ W m^{-2} and $T_a = 20$ °C; and (b) $G = 800$ W m^{-2} and $T_a = 20$ °C.

3.3. Annual simulations of single-stage and two-stage systems

The solar-ORC S-CHP system is simulated over an entire annual period with actual London UK climate data for both the single-stage and two-stage solar collector array configurations. A comparison of the annual work output and overall efficiency for the range of working fluids in the single-stage simulations are presented in Fig. 6. The best performing fluids are found to be those that showed good performance for both the high and low irradiance cases in Section 3.1, specifically R245ca, R123 and R11. The best performing fluid, R245ca, is found to deliver a maximum net annual electricity output from the ORC system of 955 kW h yr^{-1} at an optimal evaporation temperature of 117 °C. This gives an annual overall efficiency for the system of 5.64%. Averaged over the whole year, the mean (continuous) electrical power output is 109 W, however, the instantaneous electrical power output from the ORC engine during periods of operation is 403 W.

Please cite this article in press as: Freeman J et al. Working fluid selection and electrical performance optimisation of a domestic solar-ORC combined heat and power system for year-round operation in the UK. Appl Energy (2016), http://dx.doi.org/10.1016/j.apenergy.2016.04.041

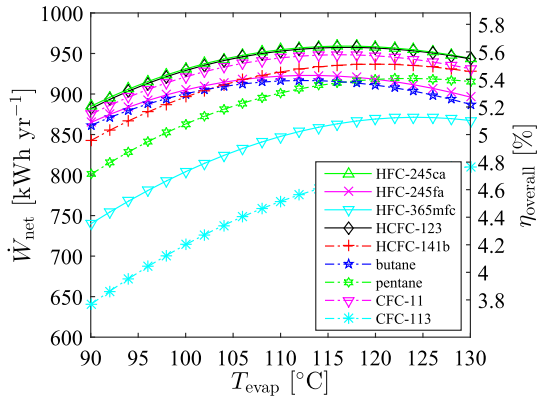

Fig. 6. Annual ORC net power output and overall efficiency for the system with the single-stage collector array configuration, as a function of evaporation temperature.

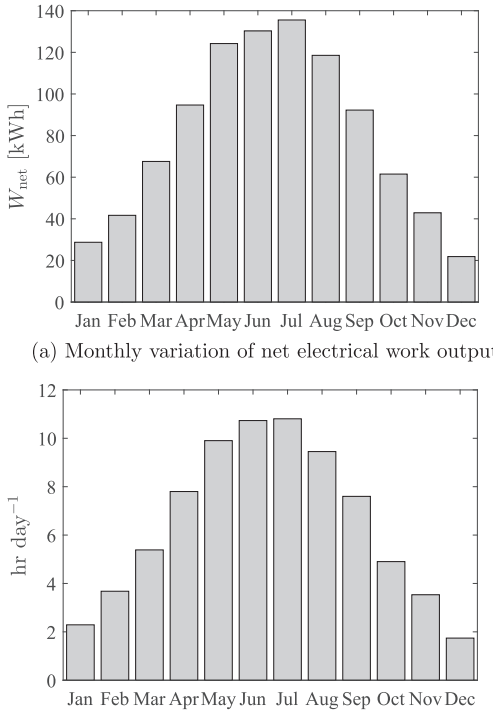

(a) Monthly variation of net electrical work output.

(b) Monthly variation of average operating hours per day.

Fig. 7. (a) ORC net electrical work output per month for the optimum working fluid/evaporation temperature combination (R245ca and T_{evap} = 117 °C), and (b) average duration of daytime operating period for each month (delivering an instantaneous net power output of 403 W ±0.3%).

The system is operational for 2370 h, or 27% of the year. It should be noted however that solar irradiance is available for only 4590 h of the year. Therefore the system is in operation for 52% of the daylight hours over the year. As shown in Fig. 7, there is a significant variation in the seasonal performance of the system due to the low solar irradiance in winter which is below the level required for the collector array to operate with a positive efficiency at the optimum system settings. Under optimum conditions, the minimum solar irradiance (direct beam plus diffuse, received by the tilted plane of the collector) under which the system is able to operate is 125 W m^{-2}. Thus it can be seen in Fig. 7a that the typical daily period of operation varies from 11 h per day in June and July, to less than 2 h per day in December, during which the nominal electrical power output from the system is 403 W. Improvements could be obtained here by incorporating a seasonal adjustment to the collector tilt angle or the system flow-rates, or focusing on the system's thermal output in the winter months. The optimal fixed flow-rates for the ORC working-fluid Pump 1 is 0.8 kg min^{-1}, giving an instantaneous shaft power output from the expander (from Eq. (8)) of 471 W. The corresponding solar fluid flow-rate circulated by Pump 3 is 11.8 kg min^{-1}. The low power output favours the use of a positive displacement expander. Scroll expanders in particular are often selected for use in ORC systems with power output < 10 kW. However the internal built-in volume ratio of scroll machines (often adapted scroll compressors) tends to be less than 5 and is limited by the number of spiral revolutions that make up the scroll assembly [53]. The volume ratio for the optimum single stage case with R245ca is 12.3, while for the two-stage case it is 15.4, therefore a single stage expansion using a scroll machine is likely to result in significant under-expansion in either case. Reciprocating expanders, on the other hand can be designed for higher pressure and volume ratios by incorporating two or more expansion stages into the same machine [54–56].

The thermal store is found to undergo an annual variation in internal energy of 1980 MJ (550 kW h). This value can be used to calculate the *minimum limit* of the volume required for a range of TES solutions. For example, for this energy to be stored by the working fluid itself in the buffer vessel as it undergoes phase change from a saturated liquid to a saturated vapour, a minimum liquid buffer volume of 13 m^3 would be required and the additional increase in volume of the vapourised fluid would also need to be accommodated in the system. This level of storage is considered prohibitive, although it may not be necessary to store this entire quantity while paying a small performance penalty. If a diurnal rather than a seasonal storage period is considered then the maximum swing in internal energy of the buffer vessel is 115 MJ (32 kW h, corresponding to a maximum continuous operating period of 12 h) which would require a buffer volume of 740 L. If a phase change material (PCM) were used instead to provide constant pressure latent thermal energy storage (TES), as proposed by Steinmann and Eck [12] and Jing et al. [14], and assuming a typical energy storage density of ~400 MJ/m^3, a PCM volume of ~5 m^3 would be required for an annual storage period and 290 L for a diurnal period (with each litre of PCM able to provide 2 min of continuous operation from the ORC engine). Thermo-chemical energy storage is a further promising solution for solar and renewables applications that has been shown to offer up to five times the energy storage density of PCM [16], thus reducing the storage volume requirement to approximately ~1 m^3 for an annual period and <100 L for a diurnal period. This solution is practically feasible, but requires the careful selection of a suitable chemical reaction to match the temperature of the specific application. Presently, the majority of thermo-chemical energy storage solutions proposed for solar thermal power plant are for temperatures in excess of 300 °C. In the authors' opinion this is an interesting direction for future research.

The ORC annual work output can be compared to the maximum annual exergy output from the solar collector array (assumed in the exergy analysis to be operating with a variable flow-rate and outlet temperature in order to deliver maximum exergy at each time-instant), which is 1830 kW h yr^{-1} at the optimum collector fixed tilt angle. Taking 955 kW h yr^{-1} as the maximum annual net ORC work output for the single-stage system, this gives an annually averaged exergy efficiency of 52%. During instances of excess solar irradiance, energy is stored in the buffer vessel that would otherwise provide superheating of the working fluid. Thus the exergy content of the fluid stream exiting the buffer vessel and entering the expander is lower in such instances than would otherwise be the case. Without the buffer vessel, the system would operate for shorter periods with a higher instaneous exergy efficiency; but would be unable to make use of solar energy received

Please cite this article in press as: Freeman J et al. Working fluid selection and electrical performance optimisation of a domestic solar-ORC combined heat and power system for year-round operation in the UK. Appl Energy (2016), http://dx.doi.org/10.1016/j.apenergy.2016.04.041

Table 3
Results from the simulations of the annually optimised systems with single-stage and two-stage collector configurations.

Parameter	Unit	Single-stage collector configuration	Two-stage collector configuration
Optimal ORC working fluid	–	R245ca	R245ca
Optimal ORC evaporation temperature	°C	117	126
Optimal ORC evaporation pressure	bar	13.5	16.3
Collector array area (Stage 1/Stage 2)	m^2	15	6.3/8.7
Net annual work output	kW h yr^{-1}	955	1070
Annually averaged net power output	W	109	122
Instantaneous/nominal net power output	W	403	481
Hours operational	h yr^{-1}	2370	2230
ORC pressure ratio	–	11.1	13.4
Pump 1 mass flow-rate	kg min^{-1}	0.8	0.9
Pump 2 mass flow-rate	kg min^{-1}	1.6	1.8
Pump 3 mass flow-rate (Stage 1)	kg min^{-1}	11.9	0.8
Pump 4 mass flow-rate (Stage 2)	kg min^{-1}	–	12.2
Mean solar collector array efficiency	–	44.0%	46.5%
ORC electrical efficiency	–	12.8%	13.6%
Annual overall efficiency	–	5.6%	6.3%
Annual exergy efficiency	–	52.2%	58.5%

during periods when irradiance intensity is insufficient to fully evaporate the working fluid and thus the annual work output would be lower.

In Table 3, the annual performance of the single-stage and two-stage collector system configurations are compared, for the optimal working fluid and evaporation temperatures. For the two-stage configuration, the relative areas of the first and second-stage collector arrays are also optimised to deliver the highest net annual electrical work output. It is found that the system with the two-stage collector array configuration is able to deliver a 12% higher net annual work output than the single-stage system. The optimal ORC evaporation temperature is also found to be 9 °C higher for the two-stage system, resulting in a 19% increase in instantaneous power output from the ORC engine; however the higher system temperatures also result in a larger number of hours (under very low irradiance conditions) for which $\eta_{sc} \leqslant 0$, and therefore the total number of operational hours per year is reduced.

The maximum annual work output reported here is also found to be 53% higher than in our earlier work [1]. The improvement can be specifically attributed to the various system modifications that have been made, as follows: (1) 4% improvement due to the choice of working fluid; (2) 10% improvement due to the choice of solar collector module; (3) 8% improvement due to the addition of the regenerator heat exchanger; and (4) 12% improvement due to the two-stage collector array configuration. The remaining improvement (a further ~20%) in power output can be attributed to the manner in which the system was simulated and optimised, specifically, the use of monthly aggregated climate data in the prior work was found to result in a non-trivial reduction in calculated power output due to non-linearity in the relationship between solar irradiance and system power output, whereas in the present analysis, the peaks in solar irradiance are more effectively represented by the hourly resolution dataset. This nonlinearity in the response and output of solar-based systems that leads to a discrepancy in the annually averaged results depending on the temporal resolution and aggregation of the input climate data has been previously identified and found to give deviations of up to a factor of two [45]; increased data aggregation was found to progressively underpredict true, full-resolution performance.

4. Conclusions

A study of domestic-scale distributed solar combined heat and power (S-CHP) systems comprising an organic Rankine cycle (ORC) engine for electrical power generation has been undertaken in order to assess their electrical performance potential in a London UK setting. The findings from this study are of relevance and applicable to similar geographical locations with significant cloud coverage, a low solar resource and restricted collector installation areas. Challenges for the design and operation of the system and its components due to the limited and intermittent nature of the UK solar resource were addressed by incorporating a working fluid buffer vessel, hypothetically sized to enable year-round operation with complete instantaneous thermal storage capacity. Thus, the system can be operated with fixed fluid flow-rates, limiting losses in component performance (efficiency, effectiveness, etc.) due to part-load operation and enabling continuous power output for longer time-periods.

Of the working fluids investigated, R245ca was found to result in the highest net annual work output for the basic single-stage S-CHP system design, which was 955 kW h yr^{-1} (64 kW h yr^{-1} per m^2 of solar collector) at a cycle evaporation saturation temperature of 117 °C. This is equivalent to a continuous power output of 109 W when averaged over the whole year. A modified S-CHP system configuration incorporating a two-stage solar collector array was found to offer an additional 12% annual work output benefit (1070 kW h yr^{-1}, or 71 kW h yr^{-1} per m^2), due to an improvement in the overall collector array efficiency. In the present design, the two-stage collector array requires an additional pump and heat exchanger and is therefore associated with an increase (approximately 5–10%) in the capital cost of the system; however, future work will explore the possibility of directly heating the ORC working fluid in the solar collector, thus omitting the need for the secondary fluid circuit.

The results presented here suggest that the considered S-CHP system operating in a UK setting can be expected to provide in the region of 32% of the typical household demand for electricity (3300 kW h yr^{-1} according to Ref. [57]). While significant, this is about half of the predicted electrical output for the same system when simulated in a southern European climate. The electrical performance can be compared to that of a mono-crystalline PV system which typically provides 110–120 kW h m^{-2} yr^{-1} in the UK climate [58], and thus for an equivalent array size (15 m^2) approximately 50% of household demand (i.e., the S-CHP solution electrical generation is 36% lower).

The advantage of the presently proposed S-CHP system is the ability to also provide water (and possibly also space) heating to the household, and to store thermal energy during times of low electricity demand for better load profile matching, as well as a considerably lower capital expenditure (by at least one-third, and

Please cite this article in press as: Freeman J et al. Working fluid selection and electrical performance optimisation of a domestic solar-ORC combined heat and power system for year-round operation in the UK. Appl Energy (2016), http://dx.doi.org/10.1016/j.apenergy.2016.04.041

arguably up to one-half) compared to an equivalent PV solution. However, overall system performance also depends on well-designed solar collectors, able to operate with high efficiency at high fluid temperatures while also making use of the large proportion of diffuse (scattered) radiation received in the UK. The new generation of evacuated flat-plate solar collector investigated here is a strong candidate technology for such an application.

At this point it is important to also discuss the economics of these systems in the context of these results. The total installed cost estimate for the basic S-CHP system presented in our earlier work was £4400–£5500 [1]. The cost of the new system optimised for maximum electrical power output is 40–50% higher as a result of the additional buffer vessel, heat exchangers, working fluid and higher efficiency solar collectors. However, due to the increased system electrical output the installed cost per unit generating capacity can be expected to be roughly the same. The revised installed cost with the additional components for increased electrical power output is expected to be in the region of £6500–£7500. As summarised in the aforementioned earlier work, an equivalent-sized (15 m^2) mono-crystalline PV array (and associated system components) has an installed cost in the region of ~£7500. The electrical output from the PV-array could also be used to provide water heating via an air source heat pump (ASHP). Domestic scale air-to-water heat pumps typically have installed costs ~£7000 [59,60] which, added to the cost of the PV system brings the total installed cost of a PV-ASHP CHP system to ~£14,500. Meanwhile, a side-by-side PV and solar hot-water (SHW) system (split 10 m^2 for PV and 5 m^2 for SHW, as in Ref. [1]) has an installed cost in the region of £9500–£10000. The total specific installed cost of the solar-ORC S-CHP system (per unit average annual power generation) is in the region ~£55–60/$W_{e,avg}$, compared to ~£73/$W_{e,avg}$ for the side-by-side PV-SHW system and ~£72/$W_{e,avg}$ for the PV-ASHP system, both of which are considerably higher. For the PV-only system, the specific installed cost is approximately ~£38/$W_{e,avg}$, however this system does not have a thermal output and thus the comparison must be with a revised specific cost value for the solar-ORC system relating only to the power generation components of the system, giving a revised figure for the solar-ORC system of ~£34–44/$W_{e,avg}$.

Thermal energy storage is a key feature of the proposed system in order to buffer the intermittent input of solar thermal energy to the system. It was found that a large volume (several cubic metres) of thermal storage material (either sensible or latent) is required in order to provide full, instantaneous buffering over the entire annual period, but that thermo-chemical storage has the potential to reduce this to 1 m^3, which is considered highly feasible. A natural direction of future work will involve an investigation of appropriate solutions for finite-sized thermal storage provision and an assessment of their effectiveness for load profile matching over diurnal as well as seasonal time-scales.

Finally, it is emphasised that this paper has focused on the performance of the S-CHP system when optimised for maximum annual electrical power generation. In CHP operation, a proportion of the solar collector heat transfer fluid may be diverted to a domestic hot water cylinder (see the system schematic in Fig. 1a), at the expense of a reduction in the thermal input to the ORC engine. Taking the water heating demand for a typical UK home to be around 2900 kW h yr^{-1} [61], the reduction in the annual electrical output from the S-CHP system in order to meet this heating demand can be expected to be in the region of 35–45%. It is noted that in the UK domestic sector both (electricity) microgeneration and renewable heat are currently promoted by government incentivisation schemes, such that both outputs would lead to financial benefits to the household beyond the direct displacement of the costs associated with the electricity taken from the grid and the natural gas used for heating (in the vast majority of cases).

Acknowledgment

This work was supported by the UK Engineering and Physical Sciences Research Council (EPSRC) [grant numbers EP/J006041/1 and EP/K502856/1]. JF gratefully acknowledges the DTG studentship awarded to him by the Department of Chemical Engineering, Imperial College London and EPSRC, without which he would not have been able to embark on this research. Data supporting this publication can be obtained on request from cep-lab@imperial.ac.uk.

References

[1] Freeman J, Hellgardt K, Markides CN. An assessment of solar-powered organic Rankine cycle systems for combined heating and power in UK domestic applications. Appl Energy 2015;138:605–20.
[2] Šúri M, Huld TA, Dunlop ED, Ossenbrink HA. Potential of solar electricity generation in the European Union member states and candidate countries. Solar Energy 2007;81(10):1295–305.
[3] Herrando M, Markides CN, Hellgardt K. A UK-based assessment of hybrid PV and solar-thermal systems for domestic heating and power: System performance. Appl Energy 2014;122:288–309.
[4] Herrando M, Markides CN. Hybrid PV and solar-thermal systems for domestic heat and power provision in the UK: Techno-economic considerations. Appl Energy 2016;161:512–32.
[5] Guarracino I, Mellor A, Ekins-Daukes NJ, Markides CN. Dynamic coupled thermal-and-electrical modelling of sheet-and-tube hybrid photovoltaic/thermal (PVT) collectors. Appl Therm Eng 2016. http://dx.doi.org/10.1016/j.applthermaleng.2016.02.056.
[6] Markides CN. The role of pumped and waste heat technologies in a high-efficiency sustainable energy future for the UK. Appl Therm Eng 2013;53(2):197–209.
[7] Markides CN. Low-concentration solar-power systems based on organic Rankine cycles for distributed-scale applications: Overview and further developments. Front Energy Res 2015;3:47.
[8] Quoilin S, Orosz M, Hemond H, Lemort V. Performance and design optimization of a low-cost solar organic Rankine cycle for remote power generation. Solar Energy 2011;85(5):955–66.
[9] Manolakos D, Kosmadakis G, Kyritsis S, Papadakis G. On site experimental evaluation of a low-temperature solar organic Rankine cycle system for RO desalination. Solar Energy 2009;83(5):646–56.
[10] Wang X, Zhao L, Wang J, Zhang W, Zhao X, Wu W. Performance evaluation of a low-temperature solar Rankine cycle system utilizing R245fa. Solar Energy 2010;84(3):353–64.
[11] Casati E, Galli A, Colonna P. Thermal energy storage for solar-powered organic Rankine cycle engines. Solar Energy 2013;96:205–19.
[12] Steinmann WD, Eck M. Buffer storage for direct steam generation. Solar Energy 2006;80(10):1277–82.
[13] Latent heat storage provides process steam. Projektinfo Brochure; 2008. <http://www.bine.info> [accessed 17/10/2015].
[14] Jing L, Gang P, Jie J. Optimization of low temperature solar thermal electric generation with organic Rankine cycle in different areas. Appl Energy 2010;87(11):3355–65.
[15] Cot-Gores J, Castell A, Cabeza LF. Thermochemical energy storage and conversion: A-state-of-the-art review of the experimental research under practical conditions. Renew Sustain Energy Rev 2012;16(7):5207–24.
[16] Hauer A. Thermal energy storage. IEA-ETSAP and IRENA technology brief.
[17] Acharya S, Bhattacharjee S. Stirling engine based solar-thermal power plant with a thermo-chemical storage system. Energy Convers Manage 2014;86:901–15.
[18] Hongois S, Kuznik F, Stevens P, Roux J-J. Development and characterisation of a new $MgSO_4$-zeolite composite for long-term thermal energy storage. Solar Energy Mater Solar Cells 2011;95(7):1831–7.
[19] Burnett D, Barbour E, Harrison GP. The UK solar energy resource and the impact of climate change. Renew Energy 2014;71:333–43.
[20] CERN's ultra high vacuum flat plate solar collector. Markets and applications; 2008. <http://indico.cern.ch> [accessed 17/10/2015].
[21] TVP Solar. HT-power product datasheet; 2013. <http://www.tvpsolar.com > [accessed 24/02/2015].
[22] TVP solar for air conditioning and cooling; 2013. <http://www.tvpsolar.com> [accessed 17/10/2015].
[23] Department of energy and climate change. Solar photovoltaics deployment in the UK; 2015. <https://www.gov.uk/government/statistics/solar-photovoltaics-deployment> [accessed 04/02/2016].
[24] Office of gas and electricity markets. Tariff tables; 2016. <https://www.ofgem.gov.uk/environmental-programmes/feed-tariff-fit-scheme/tariff-tables> [accessed 04/02/2016].

Please cite this article in press as: Freeman J et al. Working fluid selection and electrical performance optimisation of a domestic solar-ORC combined heat and power system for year-round operation in the UK. Appl Energy (2016), http://dx.doi.org/10.1016/j.apenergy.2016.04.041

[25] Calise F, d'Accadia MD, Vicidomini M, Scarpellino M. Design and simulation of a prototype of a small-scale solar CHP system based on evacuated flat-plate solar collectors and organic Rankine cycle. Energy Convers Manage 2015;90:347–63.
[26] Dow chemical company. "Dowtherm A" Heat transfer fluid. Product technical data; 1997.
[27] Perers B, Bales A. A solar collector model for TRNSYS simulation and system testing. Report of IEA SHC – Task 26: Solar combisystems.
[28] BS EN 12975-2: 2006. Thermal solar systems and components. Solar collectors. Test methods; 2006.
[29] Buonomano A, Calise F, Palombo A, Vicidomini M. Energy and economic analysis of geothermal–solar trigeneration systems: A case study for a hotel building in Ischia. Appl Energy 2015;138:224–41.
[30] Guarracino I, Freeman J, Markides CN. Experimental validation of a 3-D dynamic solar-thermal collector model under time-varying environmental conditions. In: 29th International conference on efficiency, cost, optimization, simulation and environmental impact of energy systems, Portorož, Slovenia, June 19–23.
[31] Test Report: durability, reliability and thermal performance of a solar collector according to EN 12975-2:2006. TVP solar SA MT-power v3.11. Tech. rep., University of Stuttgart, Institut für Thermodynamik und Wärmetechnik; March 2012.
[32] Incropera FP, Lavine AS, DeWitt DP. Fundamentals of Heat and Mass Transfer. John Wiley & Sons Incorporated; 2011.
[33] Wang H, Touber S. Distributed and non-steady-state modelling of an air cooler. Int J Refrigeration 1991;14(2):98–111.
[34] Quoilin S, Lemort V, Lebrun J. Experimental study and modeling of an organic Rankine cycle using scroll expander. Appl Energy 2010;87(4):1260–8.
[35] Clemente S, Micheli D, Reini M, Taccani R. Performance analysis and modeling of different volumetric expanders for small-scale organic Rankine cycles. In: ASME 2011 5th international conference on energy sustainability, Washington DC, USA. p. 7–10.
[36] Badr O, O'Callaghan P, Hussein M, Probert S. Multi-vane expanders as prime movers for low-grade energy organic Rankine-cycle engines. Appl Energy 1984;16(2):129–46.
[37] Quoilin S. Experimental study and modeling of a low temperature Rankine cycle for small scale cogeneration Master's thesis. University of Liege; 2007.
[38] Badr O, Naik S, O'Callaghan P, Probert S. Expansion machine for a low power-output steam Rankine-cycle engine. Appl Energy 1991;39(2):93–116.
[39] Bracco R, Clemente S, Micheli D, Reini M. Experimental tests and modelization of a domestic-scale organic Rankine cycle. In: 25th International conference on efficiency, cost, simulation and environmental impact of energy systems, Perugia, Italy.
[40] Saitoh T, Yamada N, Wakashima S-I. Solar Rankine cycle system using scroll expander. J Environ Eng 2007;2(4):708–19.
[41] Wang W, Wu Y-T, Ma C-F, Liu L-D, Yu J. Preliminary experimental study of single screw expander prototype. Appl Therm Eng 2011;31(17):3684–8.
[42] Quoilin S, Declaye S, Tchanche BF, Lemort V. Thermo-economic optimization of waste heat recovery organic Rankine cycles. Appl Therm Eng 2011;31(14):2885–93.
[43] Wang M, Wang J, Zhao Y, Zhao P, Dai Y. Thermodynamic analysis and optimization of a solar-driven regenerative organic Rankine cycle (ORC) based on flat-plate solar collectors. Appl Therm Eng 2013;50(1):816–25.
[44] Lecompte S, Huisseune H, Van den Broek M, De Schampheleire S, De Paepe M. Part load based thermo-economic optimization of the organic Rankine cycle (ORC) applied to a combined heat and power (CHP) system. Appl Energy 2013;111:871–81.
[45] Freeman J, Hellgardt K, Markides CN. An assessment of solar-thermal collector designs for small-scale combined heating and power applications in the United Kingdom. Heat Transfer Eng 2015;36(14–15):1332–47.
[46] ASHRAE. International weather for energy calculations (IWEC) weather files. Users manual and CD-ROM; 2001.
[47] Chen H, Goswami DY, Stefanakos EK. A review of thermodynamic cycles and working fluids for the conversion of low-grade heat. Renew Sustain Energy Rev 2010;14(9):3059–67.
[48] Rayegan R, Tao Y. A procedure to select working fluids for solar organic Rankine cycles (ORCs). Renew Energy 2011;36(2):659–70.
[49] Bao J, Zhao L. A review of working fluid and expander selections for organic Rankine cycle. Renew Sustain Energy Rev 2013;24:325–42.
[50] Oyewunmi OA, Taleb AI, Haslam AJ, Markides CN. An assessment of working-fluid mixtures using SAFT-VR Mie for use in organic Rankine cycle systems for waste-heat recovery. Comput Therm Sci: An Int J 2014;6(4).
[51] Oyewunmi OA, Taleb AI, Haslam AJ, Markides CN. On the use of SAFT-VR Mie for assessing large-glide fluorocarbon working-fluid mixtures in organic Rankine cycles. Appl Energy 2016;163:263–82.
[52] Jung D, McLinden M, Radermacher R, Didion D. Horizontal flow boiling heat transfer experiments with a mixture of R22/R114. Int J Heat Mass Transfer 1989;32(1):131–45.
[53] Quoilin S. Sustainable energy conversion through the use of organic Rankine cycles for waste heat recovery and solar applications Ph.D. thesis. Belgium: University of Liège; 2011.
[54] Guarracino I, Mathie R, Taleb A, Markides CN. An experimental analysis of a low-loss reciprocating piston expander for use in small-scale organic Rankine cycles. In: 2nd International seminar on ORC power systems, Rotterdam, The Netherlands.
[55] Imran M, Usman M, Park B-S, Lee D-H. Volumetric expanders for low grade heat and waste heat recovery applications. Renew Sustain Energy Rev 2016;57:1090–109.
[56] Lemort V, Guillaume L, Legros A, Declaye S, Quoilin S. A comparison of piston, screw and scroll expanders for small scale Rankine cycle systems. In: The 3rd international conference on microgeneration and related technologies.
[57] Office of gas and electricity markets. Typical domestic energy consumption figures factsheet; 2011. <http://www.ofgem.gov.uk> [accessed 21 May 2013].
[58] Energy Saving Trust. A buyer's guide to solar electricity panels; 2011.
[59] Staffell I, Brett D, Brandon N, Hawkes A. A review of domestic heat pumps. Energy Environ Sci 2012;5(11):9291–306.
[60] Energy Saving Trust. Air source heat pumps; 2016. <http://energysavingtrust.org.uk> [accessed 04/02/2016].
[61] Energy Saving Trust. Here comes the sun: A field trial of solar water heating systems; 2011.

Please cite this article in press as: Freeman J et al. Working fluid selection and electrical performance optimisation of a domestic solar-ORC combined heat and power system for year-round operation in the UK. Appl Energy (2016), http://dx.doi.org/10.1016/j.apenergy.2016.04.041